*Article*

*J. Mex. Chem. Soc.* **2015**, *59(3)*, 215-228

ISSN 1870-249X

# Removal of Direct Dyes with Alginic Acid

Juan Antonio Lozano-Alvarez,[1] Virginia-Francisca Marañón-Ruiz,[2]* Juan Jáuregui-Rincón,[1] Iliana Medina-Ramírez,[3] Claudio Frausto-Reyes[4] and Rogelio Salinas-Gutiérrez[5]

[1] Departamento de Ingeniería Bioquímica, Universidad Autónoma de Aguascalientes, Av. Universidad 940 Cd. universitaria, Aguascalientes, México, C.P. 20131.
[2] Departamento de Ciencias de la Tierra y de la Vida, Centro Universitario de los Lagos, Universidad de Guadalajara. Av. Enrique Díaz de León # 1144, Col. Paseos de la Montaña, Lagos de Moreno, Jalisco, México, C.P.47460.
[3] Departamento de Química, Universidad Autónoma de Aguascalientes, Av. Universidad 940 Cd. universitaria, Aguascalientes, México, C.P. 20131.
[4] Centro de Investigaciones en óptica, Unidad Aguascalientes, Prol. Constitución 607, Fracc. Reserva Loma Bonita Aguascalientes, México, C. P. 20200.
[5] Departamento de Estadística, Universidad Autónoma de Aguascalientes, Av. Universidad 940 Cd. universitaria, Aguascalientes, México, C.P. 20131.
* To whom correspondence should be addressed. Mail Adress: vmaranon@culagos.udg.mx
Telephone: 52 (474) 7424314 Ext. 66585. Fax: 52 (474) 7423678.

Received July 27,2015; Accepted November 10, 2015

**Abstract.** The interaction of Alginic acid with three direct dyes (Direct blue 1, Direct red 81, and Direct black 22) was studied. It was found that as a result of this interaction formation of adducts after addition of calcium ion, facilitates their removal from aqueous solution. Our results suggest a relationship among physico-chemical properties of each dye and its removal efficiency. The main mechanisms involved in dye removal are electrostatic interactions, hydrogen bonding and hydrophobic interactions.
**Key words:** Alginic acid, direct dyes, electrostatic interactions, hydrogen bonding, hydrophobic interactions.

**Resumen.** La interacción del ácido algínico con tres colorantes directos (azul directo 1, rojo directo 81 y negro directo 22) fue estudiada. Se encontró que como resultado de esta interacción, la formación de aductos tras la adición del ion calcio, facilita su remoción de solución acuosa. Nuestros resultados sugieren una relación entre las propiedades fisicoquímicas de cada colorante y su eficiencia de remoción. Los principales mecanismos involucrados en la remoción de colorantes son las interacciones electrostáticas, puentes de hidrógeno e interacciones hidrofóbicas.
**Palabras clave:** Ácido algínico; colorantes directos; interacciones electrostáticas; puentes de hidrógeno; interacciones hidrofóbicas.

## Introduction

It is well known that suitable dyes to be used for the textile industry should have the highest physical and chemical stability [1]. However, these properties cause considerable environmental problems when these compounds are discharged into water receptors. It has been reported that approximately ten to fifteen percent of applied dye remains in the liquor resulting from dyeing process, in addition more than 100,000 different dyes and pigments are produced worldwide with a total annual production of 700,000 metric tons per year [2], as a consequence the water pollution by these substances represents a complex challenge to resolve.

Direct dyes can be applied to different substrates (materials) such as leather, cotton, silk, cellulose and wool. This group of dyes contain in their structure, different functional groups such as azo, sulfonate, amino, nitro, and others that make a wide variety of colors possible. Due to its complex chemical structure, these compounds are difficult to metabolize by organisms encountered in the environment and when transformed through anaerobic treatments, the products generated (aromatic amines) are mutagenic and carcinogenic [3-5].

Different strategies have been used to remove direct dyes from aqueous solution, among them, advanced oxidation processes [6-13], coagulation/flocculation [14], electrochemical processes [15,16], extraction [17], inclusion in polymeric materials such as β-cyclodextrin-based polymers, and calixa(n)renes derivatives [18-23], bacterial biodegradation [24-26], decolorization with fungi and their purified enzymes [27-30], and adsorption [31-33]. However, each method has its own limitations and drawbacks such as high cost of the material used in dye removal, cost of confinement of residual products, and the high energy demand of the processes, among others.

Adsorption is an economic option that can be applied to remove direct dyes. In recent years, low cost materials such as baggase pith, rice husk, maize cob and sunflower stalks have been evaluated for the treatment (dye removal) of polluted waters [34]. Although these substrates have an acceptable capacity to remove different dyes, their adsorption efficiency is very variable, since it depends on several factors, such as, the source

of residue, the harvest season, and the treatments applied to the low cost adsorbents used in the dye removal.

Lately, it has been demonstrated that biopolymers can be used for the removal of dyes from polluted waters. Several polymers have been evaluated, among them, chitosan, chitin, cellulose, guar gum, tamarind gum, locust bean gum, wheat and corn starch, dextrin, carrageenan, pectin, alginic acid and xanthan have shown good removal capacity and high biodegradability [35-40].

Alginic acid (ALG) is a polymer produced by brown seaweed (Phaeophyceae) and bacterium (*Azotobacter vinelandii*). It is widely used in the food industry as a stabilizer, thickener and gelling agent. Its structure consists in a linear chain of β(1→4)-D-mannuronate (M) and α(1→4)-L-guluronate (G) [41]. Lozano-Alvarez *et al*. [39] reported that this polymer can be effectively used for the removal of disperse yellow 54 (DY54) from aqueous medium using the ALG and separating the ALG-DY54 adduct by acidification. It was also reported that the experimental data of the adsorption isotherms of dye/alginic acid can be best adjusted to the Zimm-Bragg model. The aim of this work is to study the performance of this biopolymer as removal agent when the adduct ALG-Dye is separated from the aqueous solution as calcium alginate gel as a consequence of the addition of calcium ion. In the same sense, we intend to expand our understanding of the interactions among different direct dyes (direct blue 1 (DB1), direct red 81 (DR81), and direct black 22 (DB22) and this polymer, taking into consideration the physicochemical properties of each dye molecule such as molecular weight, size, aggregation capacity, number and nature of functional groups which determine the differences observed in their removal efficiency with this biopolymer. In this paper, we report a careful examination of these properties of direct dyes and relate them to their interaction with ALG biopolymer, aiming to improve the efficiency of this polymer to remove direct dyes from aqueous solution.

## Results and Discussion

### Sorption studies

The removal of direct dyes by ALG was evaluated. First, the removal capacity of this polymer was studied as a function of pH and ionic strength values. Fig. 1 shows the graphics corresponding to the removal efficiencies for the following systems: (a) ALG-DB1 (Ca), (b) ALG-DR81 (Ca) and (c) ALG-DB22 (Ca) taking into consideration, different pH and ionic strength values. Fig. 1a shows that pH influences considerably the removal capacity of ALG, observing higher removal efficiencies at high pH values. Fig. 2 represents the chemical structures of dyes used in this study, it can be seen from this figure that these direct dyes have considerable structural differences. Due to its chemical structure, DB1 molecules possess a negative charge at high pH values. Despite the fact that an increase of the pH value results in a higher repulsion between DB1 and ALG molecules, the deprotonation of guluronate (in the polyGGGGG and mixed MGMGM regions of ALG) is favored and the affinity of these regions for the $Ca^{+2}$ increases.

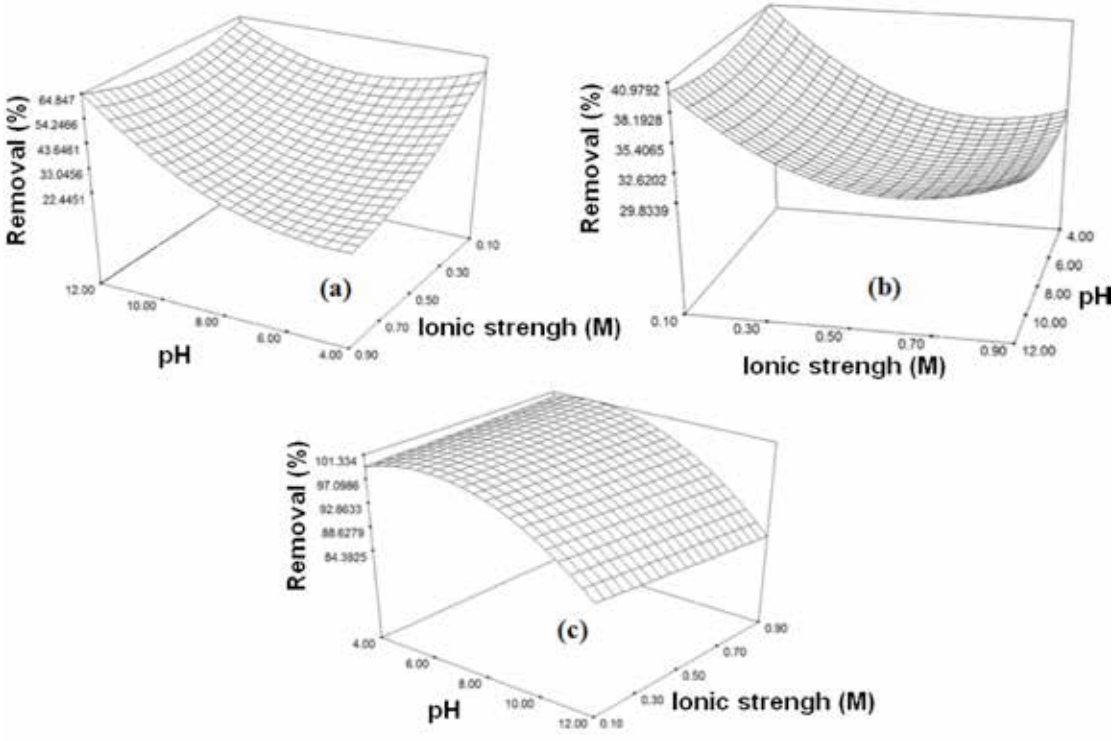


**Fig. 1.** Graphical representation of Removal efficiency as a function of pH and ionic strength for the following systems: (a) ALG-DB1 (Ca), (b) ALG-DR81 (Ca), and (c) ALG-DB22 (Ca).

In this sense, Donati *et al*. [42] have reported that the main residues involved in the formation of calcium alginate gel ALG (Ca) were the guluronate groups in the ALG molecules (poliGGGG regions), nevertheless it was found that the "mixed regions" formed by mannuronate and guluronate in alternate form (MGMGMG) also participate in the gel formation. As a consequence, we propose that there is a decrease in the repulsion between ALG-DB1 adducts when the gel is formed. In addition it is known that the poli mannuronate sequences (poliMMMM) and the MGMGMG are more flexible than the poliGGG moieties [41], and consequently we propose that when the ALG-DB1 (Ca) gel is formed the spaces between poliMMMM and MGMGMG "capture" the DB1 molecules and DB1 clusters adsorbed to the ALG molecular surface.

We previously reported [39] that high values of ionic strength promote the formation of disperse yellow 54 (DY54) aggregates in aqueous solution which increased the Van der Waals and hydrophobic interactions between this dye and the ALG molecules. In this sense Oakes and Dixon [43] have proposed that an increase in the number of aromatic rings favors the phenomenon of dye aggregation (by π-π stacking) and as can be seen in fig. 2, DB1 has two phenyl and two naphthyl rings, which contribute to form greater DB1 aggregates that can bind to ALG. In addition, the functional groups attached to the DB1 molecule (such as amino, sulfonate, methoxy and keto) can interact with the hydroxyl and carboxyl groups of ALG biopolymer through hydrogen bonding. All these contributions resulting in a considerable increase of removal efficiency (64 % at pH =12 and ionic strength I=0.9M).

On the other hand, at lower pH values the effect of ionic strength on the removal efficiency of DB1 is greater than that observed at high pH values. Although there is a decrease in the repulsion between ALG and DB1 molecules, the presence of a high salt concentration hinder the approach between these chemical species, which results in lower removal efficiencies of this dye as can be seen in fig. 1a.

Fig. 1b shows schematically the effect of pH and ionic strength on the removal efficiency of the DR81 dye by ALG. Interestingly the effect of the pH is not as strong as that observed with DB1. The structure of DR81 (Fig. 2b) indicates that this dye possesses a negative charge in a wide pH range which explains why this dye is affected less than that observed with DB1. The DR81 molecule has two sulfonate groups that have a negative charge at almost any pH value, and the hydroxyl group can be deprotonated at high pH values increasing the negative charge of this dye. However, from Fig 1b it can easily be inferred that this last deprotonation step does not have a strong effect on the removal efficiency.

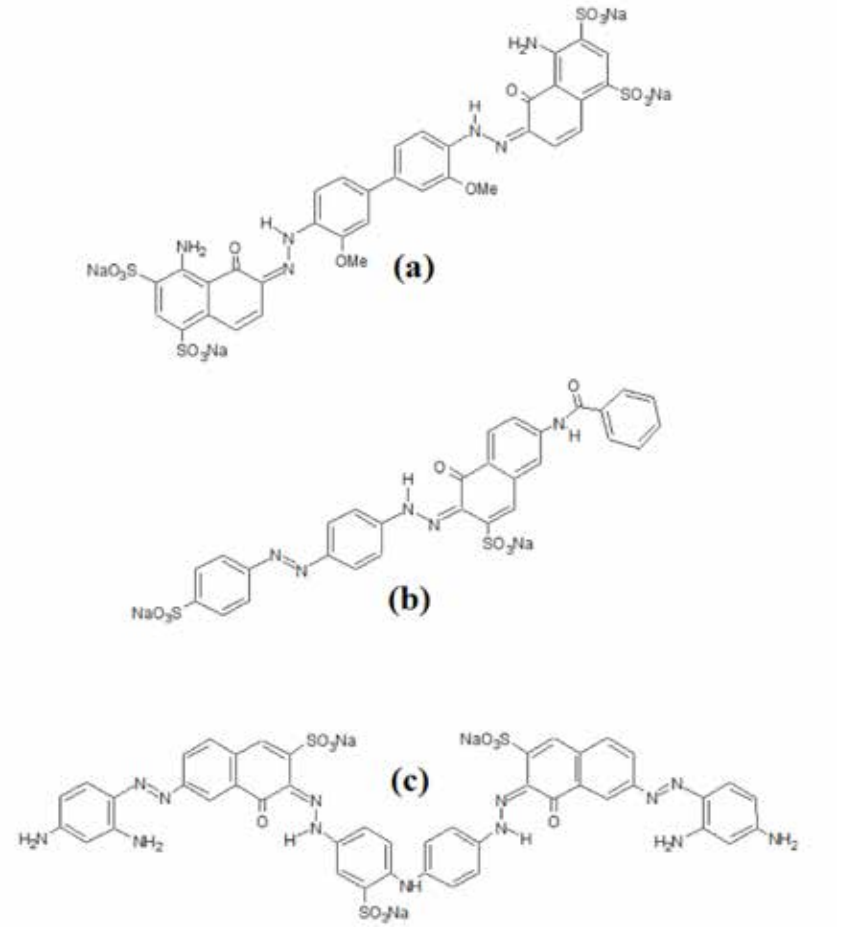


**Fig. 2.** The structure of Direct dyes: (a) Direct blue 1 (DB1), (b) Direct red 81 (DR81), and (c) Direct black 22 (DB22).

On the other hand, this figure also shows that the ionic strength causes a considerable effect on dye´s removal. This result suggests a possible hydrogen bonding and electrostatic interactions between DR81 and the ALG. The amide bond might be broken at acidic and/or basic pH values, resulting in the formation of a dye molecule with an amine group that modifies the "removal efficiency profile" of the dye. This chemical modification of the dye, leads to coulombic interactions of the dye with the ALG polymer, but also, the presence of sodium chloride, decreases the efficiency of dye removal due to the excess of $Cl^-$ and $Na^+$ ions which interact with the amino groups (in DR81) and carboxyl groups (in ALG) respectively. Conversely, a low ionic strength (I =0.1M) does not reduce ALG-DR81 interactions, resulting in a higher removal (41 % at pH = 4.0 and I = 0.1M). Although we encountered similarities in the mechanism involved in ALG-Direct dye (DB1 and/or DR81) interactions, also, some differences were encountered which are due to the smaller size and molecular weight of DR81, that can be reflected in a lower removal percentage.

Fig. 1c illustrates the influence of pH and ionic strength on the removal efficiency for the system ALG-DB22 (Ca). It is observed that the pH has a deeper effect than the ionic strength on the removal efficiency of this dye; in this sense, removal efficiencies of DB22 by ALG up to 99% can be achieved at low pH values (pH = 4). With regard to the functional groups that integrate the complex chemical structure of DB22 (shown in Fig. 2c), such functional groups will be ionized as a function of the solution pH value, in particular, at pH = 4, DB22 presents a charge with a positive value (+2) as a result of the net sum of the three sulfonate groups (each one possesses a charge of -1) and the five amino groups (contributing with an approximate charge of +5). In the same order, the ALG molecule contains guluronate and mannuronate monomers which have one carboxylate group per residue. The pKa values of mannuronate and guluronate groups are $pKa_M$ = 3.38 and $pKa_G$ = 3.65 respectively [44], this means that these groups are partially deprotonated at a pH=4 (approximately, ten percent of the carboxyl groups are ionized), in consequence there is a little attraction among ALG molecules and DB22. UV-Vis studies (see spectroscopic section) suggest a high tendency of DB22 molecules to form H aggregates due to the presence of aromatic rings (phenyl and naphthyl), high size and elevated molecular weight. This results in the adsorption of these aggregates onto the molecular surface of the ALG molecule. Interestingly the aggregation phenomenon observed in this dye is strong enough to be almost unaffected by the ionic strength. To corroborate this mechanism, solubility studies were conducted (a more elaborated discussion can be found in the IR studies section) and our results indicated a strong interaction among DB22 and ALG since this dye cannot be separated from the biopolymer after successive ethanol additions.

On the other hand, an increase in pH will favor the deprotonation of amino and hydrazone groups attached to the DB22 molecules and the ionization of carboxyl groups from ALG molecule. As a consequence a greater repulsion between DB22 and the ALG is manifested as lower removal efficiency.

## Removal Isotherms

Zimm and Bragg [45], originally proposed their theory to model the conformational transitions in proteins. Later, their theory was used in an adapted form to describe the binding of dyes and surfactants to polypeptides [46,47]. Our group [48], reported on the application of the Zimm-Bragg theory to ALG-Dye and XANT-Dye systems; It was found a respectable relationship between the experimental data and the theoretical isotherms resulting from this model.

The Zimm-Bragg theory takes into account that two processes are responsible for the aggregates formation: nucleation and aggregation. The first process (nucleation which is represented by Ku) consists in the tendency of one dye molecule to bind to a site adjacent to another one already occupied by other dye molecule on the polymer surface. The Ku magnitude is determined by the equation 1:

$$Ku = DD / (ED)\,(D), \qquad \text{Eq. (1)}$$

Where DD refers to two adjacent sites occupied by two Dye molecules and E indicates an empty site onto the biopolymer. The Cooperativity parameter U is defined as follows:

$$U = \frac{(DD)(EE)}{(DE)^2}, \qquad \text{Eq. (2)}$$

This parameter is related with the aggregation process of dye molecules bounded to the polymer. The binding coefficient (β) defined as the fraction of polymer sites occupied by dye molecules divided by the total potential sites of binding, is defined by the equation 3 showed below, where both parameters Ku and U are included.

$$\beta = \frac{1}{2}\left\{1 + \frac{s-1}{\left[(1-s)^2 + \left(\frac{4s}{u}\right)\right]^{\frac{1}{2}}}\right\}, \qquad \text{Eq. (3)}$$

With s=KuCeq, where Ceq is defined as the concentration of free dye molecules that remain in aqueous solution at equilibrium state. The parameter Ku and U are obtained from the equations 4 and 5 respectively:

$$Ceq(in\beta = 0.5) = 1/Ku, \qquad \text{Eq. (4)}$$

$$\left[\frac{d\beta}{log\,Ceq}\right] in\beta = 0.5 = U^{1/2}/4, \qquad \text{Eq. (5)}$$

Applying the equations (4) and (5) to the experimental isotherm, the Ku and U values can be obtained. By using these values as the starting ones to perform an optimization process, the theoretical parameters of Ku and U that fit with the experimental data for each system are achieved.

In Fig. 3 is represented the experimental data and theoretical isotherms obtained from equation (3) by the optimization

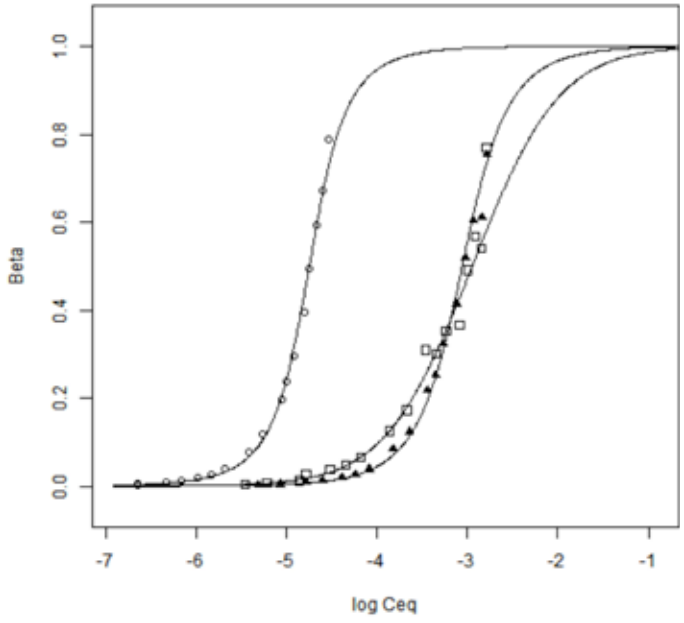


**Fig. 3.** Experimental data and theoretical Isotherms obtained from equation 3 for the following systems: Open squares (ALG-DB1 (Ca)), closed triangles (ALG-DR81 (Ca)) and open circles (ALG-DB22 (Ca)). The continuous line represents the theoretical Zimm-Bragg Isotherm for each system.

process and table 1 summarizes the Ku and U values encountered for all systems.

From Fig. 3 and table 1 it can be seen that the Ku and U values follow the order DB22 > DR81 > DB1. As mentioned before, the removal efficiency is a contribution of different factors that can be reflected in the Ku and U values. The molecular weight and size are considered as important parameters, because as bigger molecules are removed by ALG, then higher mass removal is achieved as compared to the same number of dye molecules with a smaller size and molecular weight. In this sense, within the molecules under study in this work, the largest and heaviest dye is DB22 (MW=1083.97 g $mol^{-1}$); besides, the aggregation capacity and net charge of this molecule, also influence on the Ku and U values. Jáuregui Rincón et al. [48] reported the high aggregation capacity shown by this dye due to the presence of aromatic rings and different functional groups such as sulfonate, amino, azo, keto and hydrazone which results in a net charge (in this case positive for DB22) that can be attracted by a molecule with an opposite charge (ALG). In addition, these functional groups have the ability to interact through hydrogen bonds with ALG. All these contributions result in higher nucleation and cooperativity values (Ku = 55,936 mol $Kg^{-1}$ and U = 4.1981) for the system ALG-DB22 (Ca).

It was found that Ku and U parameters were slightly higher in the ALG-DR81 (Ca) system than the values observed for the ALG-DB1 (Ca) product (ALG-DR81 (Ca): Ku = 1,142.1 mol $Kg^{-1}$ and U = 2.8409; ALG-DB1(Ca): Ku = 887.48 mol $Kg^{-1}$ and U = 0.81076. Although the size and molecular weight of DB1 are greater parameters than those corresponding to DR81, it is important to note that the removal isotherms were carried out at a pH = 4 and pH = 12 for DR81-ALG (Ca) system and ALG-DB1 (Ca) respectively and this caused a higher negative charge in the DB1 molecules (approximately -4) than the DR81 dye (-2) (see Fig. 2). As a result of this difference in negative charge, we propose that there is a minor repulsion between the DR81 and ALG molecules than that resulting from the DB1 and ALG. Notwithstanding the addition of calcium ions which decreases the repulsion between the ALG and the dyes, it seems to be that it is not enough to favor a higher nucleation and aggregation in the DB1 molecules. From the $R^2$ values, one can conclude that the Zimm-Bragg model describes in a good manner the experimental values in the three systems, despite the existence of moderate average relative error values due to experimental uncertainties arising from the high viscosity and slight turbidity of the solutions of each system.

Recently it was reported the Ku and U values of the ALG-DY54 (Ca) system (where DY54 denotes disperse yellow 54 dye) [48]. In our work, it was found that Ku = 685 mol $Kg^{-1}$ and U = 200, which implicates a lower nucleation capacity than the dyes used in this work, this can be attributed to a lower molecular weight and size of the DY54 molecules. In addition the basic pH, at which removal experiments were performed (pH=11.4), favored the repulsion forces between both the ALG and DY54 molecules. Conversely the high value of the cooperativity constant exceeds the values obtained for DB22, DR81, and DB1 compounds, it was reported that a dye precipitation in conjunction with the formation of a calcium hydroxide powder increased dramatically the value of this parameter. Interestingly from these results we can deduce that the ALG biopolymer has the capacity to reduce the dye concentration in an aqueous phase but also has the ability to remove insoluble materials such as $Ca(OH)_2$, cellulose, and kaolin as was reported recently [49-51].

**Table 1.** Parameters obtained when Zimm-Bragg model is applied to experimental data of ALG-Dye (Ca) systems.

| System | ALG-DB1(Ca) | ALG-DR81(Ca) | ALG-DB22(Ca) |
|---|---|---|---|
| Ku (mol $Kg^{-1}$ ) | 887.48 | 1,142.1 | 55,936.0 |
| U | 0.8107 | 2.8409 | 4.1981 |
| $R^2$ | 0.9499 | 0.9903 | 0.9941 |
| ARE [a] | 11.343 | 8.3392 | 14.2290 |

a: Average relative error.

## Spectroscopic studies

### UV-Visible studies

Analysis of the interaction of ALG polymer and direct dyes was followed by means of UV-Vis spectroscopy. In Fig. 4 it can be easily seen the influence of the pH value and the absorption spectrum of DB1 in aqueous solution. It is observed that in the pH range from 4 to 9, the absorption maximum of DB1 keeps constant; however, when pH is raised (pH = 12), a shift in the absorption maximum of the solution is observed (from λ=618 nm at pH=9 to λ=584 nm at pH=12). This change is due to a deprotonation of the dye molecule and it indicates that the hydrazone tautomer of DB1 predominates in aqueous solution, the spectrum obtained at pH=12 corresponds to the common anion as was found by Abbot et al. [52].

It was reported a natural tendency of different dyes to form H aggregates and it was also found that structural characteristics such as molecular weight, size, and the presence of different chemical groups favor this aggregation phenomenon [43, 53-57]. In order to investigate the aggregation capacity of DB1 at a pH=12, the spectra of this dye were acquired at different concentration values (1-500 ppm). Our results are represented in Fig. 5. From this figure we can see that the maximum absorption (λ=584 nm) does not change as a function of concentration. Abbot *et al*. [58] reported that DB1 has the ability to form dimers and trimers at ionic strength values similar to those used in this study. Besides, it was also reported that at pH 13, this dye forms the "common anion" and the planarity of this new chemical specie is similar to the hydrazone form of the DB1 at pH=7.0 [52]. From here, we can discuss that in our study, DB1 forms the common anion at pH=12 and that such anion does not have additional tendency to form aggregates when the concentration of the dye is increased. At this pH value the negative charge from this common anion promotes a considerable repulsion force between dye molecules, decreasing the aggregation capacity of this dye. However, these results do not exclude the existence of H aggregates before the pH was adjusted to a pH=12 and it is possible that DB1 aggregates involving "common anions inside them" still remain at this pH value and the UV-Visible studies only reveal that these anionic forms of DB1 do not form additional aggregates when the concentration of DB1 is increased.

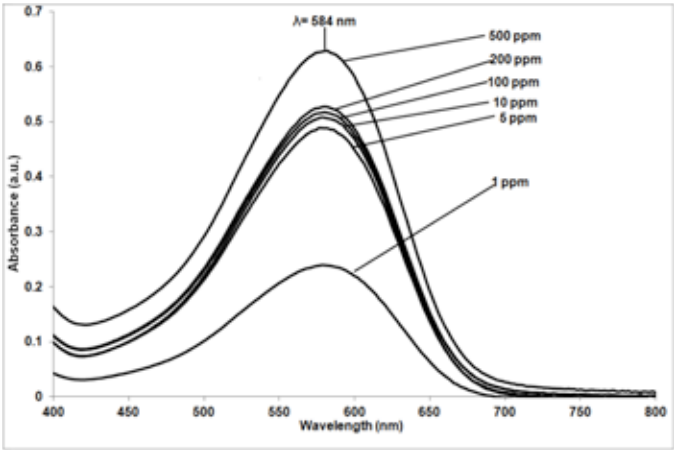


**Fig. 5.** UV-Visible absorption spectrum of DB1 in an aqueous solution at different concentration values (pH = 12.0).

Additionally the absorption electronic spectra of DB1 solutions at different concentrations were obtained in the presence of ALG (1% w/v) in an aqueous environment at a pH=12 (Fig. 6). As can be seen in this figure, the presence of ALG causes a shift from 584 nm (in the absence of ALG) to 578 nm at concentration values of DB1 as low as 5 $mgL^{-1}$, these results indicate that ALG promotes the aggregation of DB1 molecules.

Pal and Mandal [36] found that potassium alginate induced a large blue shift (Δλ = 125 nm) when interacted with 1,9-dimethylmethylenblue (DMB) in aqueous solution, such displacement of $\lambda_{max}$ was explained as a strong tendency of DMB to form H aggregates in the presence of ALG in its potassium salt form. This research group attributes H aggregate formation of DMB to its planar structure which favors the π-π stacking between dye molecules. As was mentioned before the presence

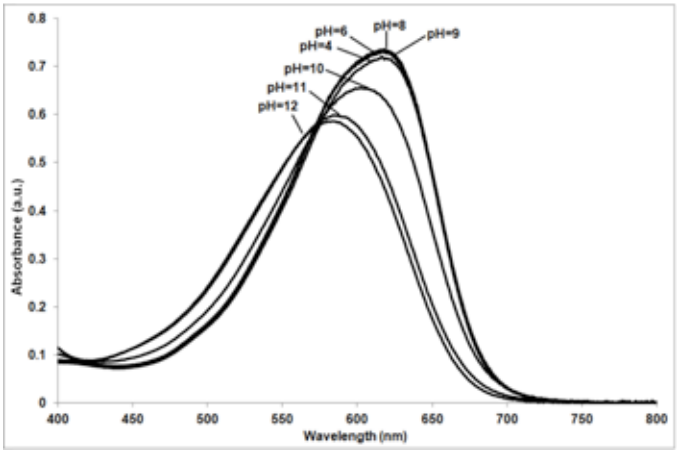


**Fig. 4.** UV-Visible absorption spectrum of DB1 in an aqueous solution at different pH values.

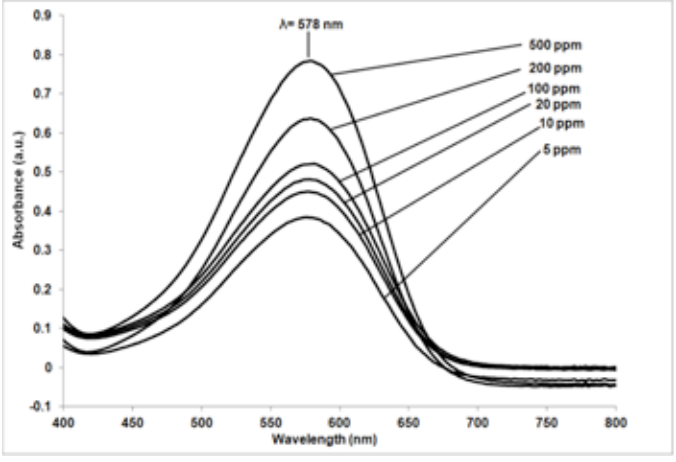


**Fig. 6.** UV-Visible absorption spectrum of DB1 at different concentration values in the presence of ALG (1 % *w/v*, pH = 12.0).

of aromatic rings in the dye molecules promotes H aggregation and it was even found that naphthyl rings were more effective in the π-π stacking between adjacent dye molecules than phenyl rings. Although the DB1 molecules are found as "common anionic forms", they have a planar geometry and both phenyl and napthyl rings attached to DB1 dye favor the subsequent formation of H aggregates. In addition to the hydrogen bonding interaction between the functional groups attached to DB1 (amino, sulfonate, methoxy and hydrazone) and hydroxyl and carboxyl groups from ALG, we propose the existence of Yoshida´s interactions [59] between the polysaccharide hydroxyl groups and the aromatic rings of DB1 molecules which results in the experimental blue shift of Δλ=6 nm. This displacement suggests a little rearrangement in the DB1 molecules, from an unstable form (soluble common anion) to a more stable chemical species, probably trimers of DB1 in their anionic form adsorbed to ALG surface but with a lesser overlapping than that observed in neutral conditions reported by Abbot *et al*. [58]. After the addition of calcium ion (as chloride salt) to ALG-DB1 complex in an aqueous medium, it was observed a new hypsochromic shift from 578 to 560 nm (Fig. 7). The addition of the calcium ion causes a reduction in the repulsion forces acting between ALG and DB1 molecules and promotes a conformational change in the ALG molecules when the calcium alginate is formed, providing a better overlapping in DB1 adjacent molecules "trapped" in the network. This change is manifested in the DB1 electronic absorption spectrum as a displacement from $\lambda_{max}$=578 nm to λmax=560 nm. From these results we can infer that DB1 molecules have a low tendency to aggregate at basic conditions (pH=12) and the presence of the ALG and calcium ions in the ALG-DB1 (Ca) adduct reinforces the π-π stacking interactions in the DB1 molecules.

In the fig. 8 it is depicted the electronic absorption spectra of DR81 ($1*10^{-5}$ M) at different pH values. From this figure, it can be seen that $\lambda_{max}$ is located at $\lambda_{max}$= 512 nm in the pH range from 2 to 8. When pH is increased, a shift in $\lambda_{max}$ (from 512 nm to 560 nm) is observed when the pH is located at pH = 11.4. This shift occurred as a consequence of the deprotonation of the hydrazone form of this dye suggesting the presence of this tautomeric form in aqueous solution.

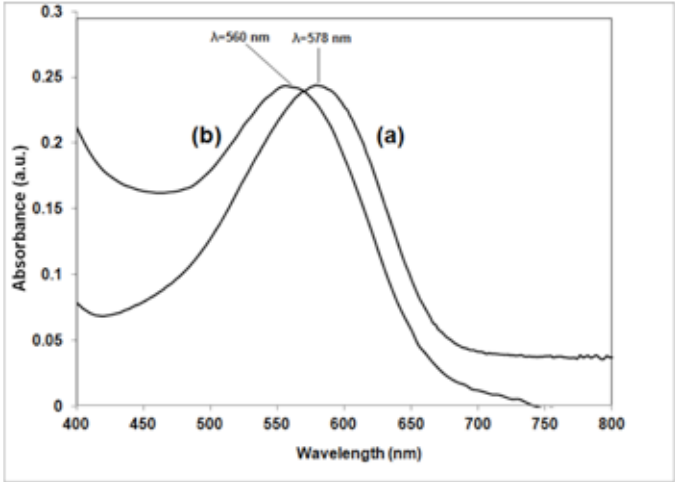


**Fig. 7.** UV-Visible absorption spectrum of: (a) ALG-DB1 (200 mg $L^{-1}$ of dye concentration, pH = 12), and (b) ALG-DB1 (Ca) gel (same conditions and 5% w/v of calcium chloride solution was added).

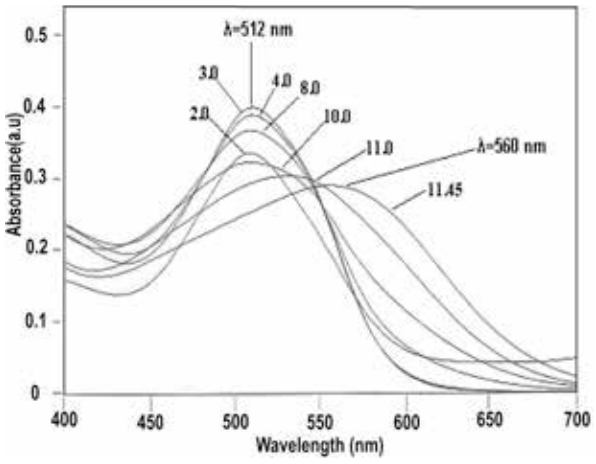


**Fig. 8.** UV-Visible absorption spectra of DR81 ($1*10^{-5}$ M) at different pH values.

Fig. 9 shows the spectra of DR81 at different concentration values (5-100 mg $L^{-1}$, pH = 4), a slight shift from 512 nm (5 mg $L^{-1}$) to 509 nm (100 mg $L^{-1}$) was observed when the concentration of this dye was increased. This small decrease in $\lambda_{max}$ was not as big as that observed in DB1, suggesting that at acidic conditions the aggregation ability of DR81 is lower than that observed with DB1. In addition, it was observed similar spectra of DR81 (data not shown), when solutions with the same dye content in the presence of ALG (1% w/v) were obtained, suggesting that ALG molecule does not have any influence in an additional formation of DR81 aggregates, due to repulsion forces among this biopolymer and DR81 and the presence of weaker interactions experimented by both the ALG and DR81 molecules.

On the other hand, it was found that the addition of calcium chloride to ALG-DR81 resulted in a gel formation and a blue shift from $\lambda_{max}$=509 nm to $\lambda_{max}$=505 nm was observed (data not

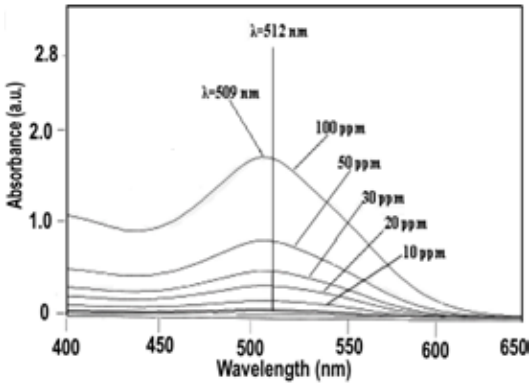


**Fig. 9.** UV-Visible absorption spectrum of DR81 in an aqueous solution at different concentration values (5-100 $mgL^{-1}$, pH = 4.0).

shown). We propose that in an analogous manner to ALG-DB1(-Ca) system, the formation of the gel induced by $Ca^{+2}$ decreases the coulombic repulsions between DR81 and ALG molecules and it is allowed that the region MGMGM and poliMMMM act in a similar way as was proposed before with the DB1 dye, but in a lesser extent. This difference in "calcium induction shift" can be qualitatively measured by the $\Delta\lambda$, that can be defined as the difference in nanometers between $\lambda_{max}$ found in the ALG-Dye system without $Ca^{+2}$ and after the addition of this ion, which has a value of $\Delta\lambda$=18 nm in the ALG-DB1 (Ca) adduct and $\Delta\lambda$=4 nm for ALG-DR81 (Ca) system. The differences observed in the $\Delta\lambda$ values can be interpreted in terms of overlapping efficiency in both dyes, namely, in aqueous environment at basic pH values the DB1 molecules cannot form aggregates but adsorption to the ALG molecule surface induces a little overlapping between aromatic rings belonging to adjacent DB1 molecules, furthermore the formation of the ALG-DB1 (Ca) gel promotes this interaction ($\pi$-$\pi$ stacking) and a newer hypsochromic shift is observed. On the other hand, we do believe that DR81 molecules are already stacked and in consequence they are forming H aggregates in an acidic aqueous solution, then an increase in the dye concentration only promotes a small aggregation.

From Fig. 2(c), it can be seen that the DB22 molecule has both, azo and hydrazone tautomeric forms and in consequence this dye can show the properties of these two tautomers. It was reported the electronic absorption spectra of DB22 at different pH values [48], and it was found that in the pH range of 2-8.3 the spectra were similar (with a $\lambda_{max}$=467 nm) suggesting that there was not a possible deprotonation step, but an increase in the basicity to pH = 10.4 caused a red shift to $\lambda_{max}$=590 nm which revealed the presence of "common anion" coming from the azo and hydrazone tautomers of DB22 dye. Based on UV-Visible data, it was discovered that DB22 forms H aggregates as a consequence of its great molecular weight and size, high number of naphthyl and phenyl rings, which affect the aggregation ability of this dye. In spite of the presence of sulfonate groups attached to the DB22 molecule, this compound has a higher ability to form H aggregates because these groups are oriented in such manner that the repulsion between them is minimal and the stability of DB22 aggregate is remained. UV-Visible spectra of DB22 showed that this biopolymer does not cause any influence in the DB22 spectrum in aqueous medium, this is in accordance with the experimental results observed with the DR81. The basic structural components of ALG molecules are the guluronate and mannuronate residues which are partially ionized and the DB22 molecule has a positive charge (approximately +2 at pH=4.0), the adsorption of DB22 aggregates did not cause any change in the electronic structure of the dye. These findings suggest that the DB22 "clusters" are highly stable and only can be disaggregated by deep changes in pH (basic pH values) due to formation of the common anion from both azo and hidrazone forms of this dye. We evaluated the effect of addition of calcium ion to the aqueous solution of ALG-DB22 complex (pH=4.0) by UV-Visible spectroscopy (data not shown); as observed for the previously discussed systems, a "blue shift" was observed in the absorption electronic spectrum of DB22 from $\lambda_{max}$=467 nm to $\lambda_{max}$=452 nm in the ALG-DB22 (Ca) adduct, resulting a shift $\Delta\lambda$=15 nm which suggests an additional rearrangement of the aggregates formed by DB22 molecules into the network produced in the gel. Braccini and Perez [41] have proposed that the gel formation of calcium alginate is carried out in two sequential steps: (1) the ALG dimer formation caused by calcium ions and (2) the subsequent interactions between these dimers. When the first step is performed, the dimers have diminished their negative net charge (the egg box model reviewed by Braccini and Perez includes four guluronate residues by each calcium ion, resulting in a net charge of -2 which is lower than -4 encountered in ALG without $Ca^{+2}$). In consequence, the repulsion among the sulfonate groups included in the DB22 molecules adsorbed into the ALG is decreased and the aggregation of the DB22 molecules on the surface of the dimers of ALG-$Ca^{+2}$ is favored. Afterwards, the second step involves an unspecific interaction mainly mediated by the electrostatic interactions between the ALG dimers and as a consequence a stable network of calcium alginate is formed. In addition, we propose an "entrapment or capturing mechanism" of the DB22 "clusters" in the regions of poliMMMM and MGMGMG sequences which have a weak affinity in the bonding of Ca(II), their flexibility allow to "trap" some aggregates of the DB22 into the gel as a consequence, a high removal efficiency value is obtained.

## Infrared and Raman studies

In order to have a better knowledge of the systems that are formed within the ALG (Ca) gel, we analyze these adducts by

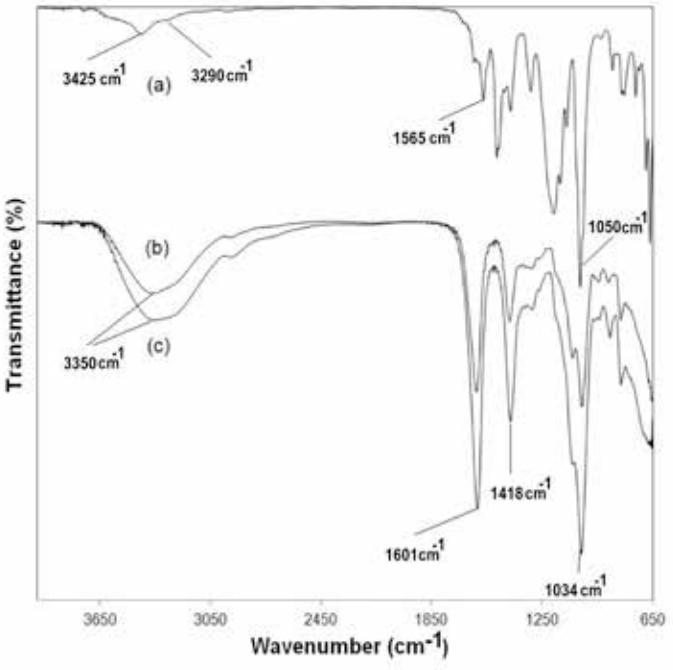


**Fig. 10.** FT-IR spectra of: (a) the DB1 dye, (b) calcium alginate ALG (Ca), and (c) the ALG-DB1 (Ca) adduct.

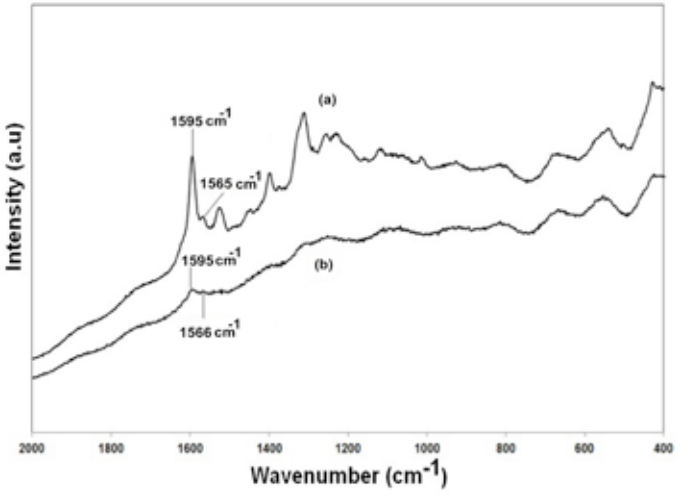


**Fig. 11.** Raman spectra of: (a) the DB1 dye, (b) and the ALG-DB1 (Ca) adduct.

Infrared (IR) and Raman spectroscopy. Infrared and Raman spectra of the DB1 dye, calcium alginate and ALG-DB1 (Ca) adduct, are depicted in figs. 10 and 11 respectively, and their data are contained in table 2.

The FT-IR spectrum of DB1 shows the typical symmetrical and asymmetrical vibrations of a primary amine located at 3425 cm $^{-1}$ and 3290 cm$^{-1}$ respectively, supporting the presence of the amino group in this dye (see also fig. 2). The signal located at 1565 cm$^{-1}$ is assigned to $_{\nu}$(C=N) from the hydrazone tautomer and the one at 1045 cm$^{-1}$ refers to $_{\nu}$(C-O) derived from methoxy groups attached to DB1 molecule. These bands may be theoretically found in the FT-IR spectrum of the ALG-DB1(Ca) spectrum (Fig. 10 c), however the presence of a broad band centered at 3350 cm$^{-1}$ corresponding to hydrogen bonding "band" prevents to detect the typical amino vibration signals (see table 2). In the same manner, the peak corresponding to $_{\nu}$(C=N) does not appear in the spectrum of ALG-DB1 (Ca) because this signal is overlapped with the asymmetrical vibration peak $_{vas}$(COO) located at 1601 cm$^{-1}$ in the ALG-DB1 (Ca) adduct, and as can be seen in the table 2, the $_{\nu}$(C-O) stretching signal suggesting the presence of the methoxy groups from DB1 is immersed in the signal of the ALG (Ca) spectrum that possesses a similar peak due to the presence of the C-O bonds from the sugar residues in its structure (see fig. 10b). From the figs. 10b and 10c, it can be affirmed that these spectra are very similar and it was necessary to obtain the Raman spectra of these compounds to confirm the presence of DB1 in the ALG-DB1 (Ca) compound.

In fig. 11 the Raman spectra of DB1 (11a) and ALG-DB1 (Ca) adduct (11b) are depicted. Unfortunately the Raman spectrum of ALG (Ca) showed a high fluorescence and it was not possible to make a peak assignation from it. Despite the low amount of DB1 in the compound ALG-DB1 (Ca), it can be observed two peaks located at 1595 cm$^{-1}$ and 1566 cm$^{-1}$ which were assigned to the stretching $_{\nu}$(C=C) from phenyl rings and $_{\nu}$(C=N) from the hydrazone tautomer respectively in accordance with Abbot et al. [60,61], confirming the presence of this dye in the ALG-DB1 (Ca) adduct (see table 2).

Table 3 summarizes the principal FT-IR and Raman signals found in the spectra of the ALG (Ca), DR81, and ALG-DR81 (Ca) compounds. The FT-IR data suggest that the main peaks of the DR81 spectrum are immersed into the spectrum of the ALG-DR81 (Ca) adduct as a result to the similarity in vibration frequencies of their functional groups. For instance the hydrogen bonding region is overlapping the band corresponding to $_{\nu}$(NH) from DR81 in its hydrazone form and the ν(C=O) from the amido group of this dye was overlapped with the broad asymmetrical vibration of the carboxylate from the ALG (Ca) compound. On the other hand, Raman signals indicate the presence of DR81 in the ALG-DR81 (Ca) adduct without ambiguity. The peak located at 1595 cm$^{-1}$ and those found in the range 1117-1135 cm$^{-1}$ were assigned to $_{\nu}$(C=C) from the phenyl rings and $_{\nu}$(-$SO_3$) from the sulfonate groups respectively. Moreover the presence of the peaks at 1564 cm$^{-1}$ and 1444 cm$^{-1}$ were attributed to the hydrazone and azo tautomers respectively in

**Table 2.** FT-IR and Raman data of ALG (Ca), DB1, and ALG-DB1 (Ca) compounds.

| FT-IR Signals | ALG (Ca) | DB1 | ALG-DB1 (Ca) | Observations |
|---|---|---|---|---|
| $_{\nu}$(OH) | 3350 cm$^{-1}$ | | 3350 cm$^{-1}$ | Suggests the presence of hydrogen bonding. |
| $\nu_{asym}$(COO) | 1602 cm$^{-1}$ | | 1601 cm$^{-1}$ | |
| $\nu_{sym}$(COO) | 1420 cm$^{-1}$ | | 1418 cm$^{-1}$ | |
| $_{\nu}$(C-O) | | 1045 cm$^{-1}$ | 1034 cm$^{-1}$ | Signal of DB1 is overlapped by ALG (Ca) signal. |
| $_{\nu}$(C=N) from hydrazone tautomer | | 1565 cm$^{-1}$ | It is not detectable | |
| $\nu_{asym}$(NH) | | 3425 cm$^{-1}$ | Not observable | Broad hydrogen bonding band prevents detection of this signal. |
| $\nu_{sym}$(NH) | | 3290 cm$^{-1}$ | Not observable | The same as above. |
| Raman Signal | | | | |
| $_{\nu}$(C=N) from hydrazone tautomer | | 1565 cm$^{-1}$ | 1566 cm$^{-1}$ | This signal confirms the presence of DB1 in ALG-DB1 (Ca). |
| $_{\nu}$(C=C) from phenyl rings | | 1595 cm$^{-1}$ | 1595 cm$^{-1}$ | This signal confirms the presence of DB1 in ALG-DB1 (Ca). |

**Table 3.** FT-IR and Raman data of ALG (Ca), DR81, and ALG-DR81 (Ca) compounds.

| FT-IR Signals | ALG (Ca) | DR81 | ALG-DR81 (Ca) | Observations |
|---|---|---|---|---|
| $_{v}$(OH) | 3440 cm$^{-1}$ | 3444 cm$^{-1}$ | 3442 cm$^{-1}$ | Hydrogen bonding still exists in ALG-DR81 (Ca). |
| $\nu_{asym}$(COO) | 1618 cm$^{-1}$ | | 1620 cm$^{-1}$ | A slightly change in vibration frequency. |
| $\nu_{sym}$(COO) | 1424 cm$^{-1}$ | | 1424 cm$^{-1}$ | Without changes |
| $_{v}$(C=O) | | 1602 cm$^{-1}$ | 1620 cm$^{-1}$ | Signal of DR81 is overlapped by $_{vas}$(COO)signal from ALG (Ca) in ALG-DR81 (Ca). |
| Raman Signal | | | | |
| $_{v}$(C=C) from phenyl rings | | 1595 cm$^{-1}$ | 1595 cm$^{-1}$ | This signal confirms the presence of DR81 in ALG-DR81 (Ca). |
| $_{v}$(C=N) from hydrazone form | | 1563 cm$^{-1}$ | 1564 cm$^{-1}$ | This signal suggests the presence of hydrazone form in ALG-DR81 (Ca) compound. |
| $_{v}$(N=N) from azo tautomer | | 1443 cm$^{-1}$ | 1444 cm$^{-1}$ | This signal suggests the presence of azo form in ALG-DR81 (Ca) compound. |
| $_{v}$(-$SO_3$ ) | | 1133 and 1117 cm$^{-1}$ | 1135 and 1120 cm$^{-1}$ | Both signals suggest and confirm the presence of DR81 in ALG-DR81 (Ca). |

accordance with Silverstein and Milton [62], Armstrong *et al*. [63] and Biswas and Umapathy [64]. These results indicate that DR81 is found in the ALG-DR81 (Ca) adduct in both tautomeric forms.

Table 4 shows the compilation of the principal FT-IR and Raman signals found in the spectra of the ALG (Ca), DB22, and ALG-DB22 (Ca) compounds. From the FT-IR data it can be seen that some signals were overlapped in a similar way that occurred in the ALG-DR81 (Ca) system, mainly the presence of peaks from the ALG (Ca) compounds prevent the detection of the DB22 signals in the spectrum data of ALG-DB22 (Ca). The symmetrical and asymmetrical vibrations of the amino group attached to DB22 ($_{vas}$(NH)=3,380 cm$^{-1}$ and $_{vs}$(NH)=3260 cm$^{-1}$) are immersed in the broad hydrogen bonding band observed in the ALG-DB22 (Ca) system. In the same manner, the bands located at 1622 cm$^{-1}$ and 1626 cm$^{-1}$ assigned to $_{v}$(C=O) from the hydrazone tautomer of the DB22 are overlapped with the asymmetrical vibration of the carboxylate group from ALG

**Table 4.** FT-IR and Raman data of ALG (Ca), DB22 and ALG-DB22 (Ca) compounds.

| FT-IR Signals | ALG (Ca) | DB22 | ALG-DB22 (Ca) | Observations |
|---|---|---|---|---|
| $_{v}$(OH) | 3450 cm$^{-1}$ | 3444 cm$^{-1}$ | 3350 cm$^{-1}$ | Hydrogen bonding still exists in ALG-DB22 (Ca). |
| $\nu_{asym}$(COO) | 1632 cm$^{-1}$ | | 1621 cm$^{-1}$ | A slight change in vibration frequency. |
| $\nu_{sym}$(COO) | 1439 cm$^{-1}$ | | 1434 cm$^{-1}$ | A slight change in vibration frequency. |
| ν(C-O) | 1032 cm$^{-1}$ | | 1037 cm$^{-1}$ | A slight change in vibration frequency. |
| $\nu_{asym}$(NH) | | 3380 cm$^{-1}$ | Not observable | Broad hydrogen bonding band prevents the detection of this signal. |
| $\nu_{sym}$(NH) | | 3260 cm$^{-1}$ | Not observable | Same as above. |
| $_{v}$(C=O) | | 1626 and 1622 cm$^{-1}$ | 1621 cm$^{-1}$ | Signal of DB22 is overlapped by $_{vas}$(COO) signal from ALG (Ca) in ALG-DB22 (Ca). |
| Raman Signal | | | | |
| $_{v}$(C=C) from phenyl rings | | 1608 cm$^{-1}$ | 1609 cm$^{-1}$ | This signal confirms the presence of DB22 in ALG-DB22 (Ca). |
| $_{v}$(C=N) from hydrazone tautomer | | 1554 cm$^{-1}$ | 1554 cm$^{-1}$ | This signal suggests the presence of the hydrazone form in ALG-DB22 (Ca) compound. |
| $_{v}$(N=N) from azo tautomer | | 1423 cm$^{-1}$ | 1420 cm$^{-1}$ | This signal suggests the presence of the azo form in ALG-DB22 (Ca) compound. |
| $_{v}$(C=C) from naphthyl rings | | 1240 cm$^{-1}$ | 1241 cm$^{-1}$ | This signal confirms the presence of DB22 in ALG-DB22 (Ca). |
| $_{v}$(-$SO_3$) | | 1166 cm$^{-1}$ | 1170 cm$^{-1}$ | Same as above. |

(Ca) in the ALG-DB22 (Ca) adduct, which made it difficult the assignment of these characteristic peaks of the DB22. Unlike the FT-IR data, the Raman signals show the presence of the DB22 in the ALG-DB22 (Ca) adduct. The (C=C) vibrations from the phenyl and naphthyl rings from DB22 were detected at 1609 $cm^{-1}$ and 1241 $cm^{-1}$ respectively and the presence of the sulfonate groups was observed as a peak found at 1170 $cm^{-1}$ in the ALG-DB22 (Ca) compound. In the same way, the presence of two peaks located at 1554 $cm^{-1}$ and 1420 $cm^{-1}$ suggest that DB22 exist as hydrazone and azo tautomers in the ALG-DB22 (Ca) (see fig. 2).

On the other hand, we performed some solubility tests of all the ALG-Dye (Ca) products with ethanol and interestingly encountered that the amount of dye released to the ethanol phase followed this order: DB1~DR81>DB22. In this sense the ALG-DB1 (Ca) and ALG-DR81 (Ca) released similar amounts of the respective dye, in contrast only traces of DB22 was encountered when ethyl alcohol was added to the ALG-DB22 (Ca). These results in conjunction with the sorption and spectroscopic studies suggest that the affinity between these dyes and the alginate molecule is different and is dependent on the structural features such as molecular weight, size, number, and nature of functional groups attached to the dye molecules of these three dyes, suggesting the main interactions involved in their removal with the ALG biopolymer. In the case of DB1 the presence of two phenyl and two naphthyl rings promotes the formation of H aggregates which interact with ALG through hydrophobic interactions and the functional groups such as amino, sulfonate, methoxy and keto form hydrogen bonds with the hydroxyl and carboxyl groups of the ALG molecule (see fig. 2). In the case of DR81 dye, the molecular weight, size and number of aromatic rings are lower than that observed with DB1, but the interactions observed with ALG are similar than those found in the system ALG-DB1 (Ca) but in lesser extent. It is important to mention that both systems, the ALG-DB1 (Ca) and ALG-DR81 (Ca) exerted some degree of repulsion with ALG, as in consequence lower removal efficiencies were observed.

In the opposite case, the presence of different functional groups attached to DB22 molecule (amino, sulfonate, azo and hydrazone tautomers) resulted in a positive charge in the molecules of this dye under the experimental conditions, in despite of the low deprotonation of ALG molecules, DB22 molecules and aggregates were attracted to ALG molecules. In addition, the DB22 dye has the higher molecular weight of all three dyes and posses two naphthyl and four phenyl rings favoring the aggregation phenomenon, thus hydrophobic interaction between the aggregates formed and the ALG molecules can be expected. All these findings result in the higher removal efficiency observed for this system. Furthermore the entrapment ability of the ALG polymer when jellified as a calcium salt and the decrease effect in the repulsion between ALG and dyes enhanced the removal efficiency in all of the in all of the systems.

In conclusion the study of the removal of three direct dyes (direct blue 1, direct red 81, and direct black 22) with alginic acid showed considerable differences in the values of dye removal efficiencies, finding the following order: ALG-DB22 (Ca)> ALG-DB1 (Ca) > ALG-DR81 (Ca). These findings suggest a relationship among physical chemical features of each dye and its removal efficiency. The main factors involved in this removal process were the aggregation capacity, the charge of each dye molecule resulting from the presence of different functional groups and the capacity of interact with ALG molecule through electrostatic interactions, hydrogen bonding and hydrophobic interactions. In addition, ALG polymer "traps" both aggregates and dye molecules when a gel is formed after the addition of calcium salt to polymer-dye adduct solution.

Moreover, more experimental work need to be done to find a deeper knowledge among the direct dye structure and its removal efficiency from aqueous solution using ALG, due to environmental importance of the direct dyes.

## Experimental

### Materials and Methods

Chemicals. The dyes DB1 and DR81 was purchased from Sigma-Aldrich and were used as received. DB22 was purchased as commercial mixture (Mardupol Co.). The purified DB22 dye was obtained by column chromatography (silica gel 60) using methanol as reported by Jáuregui-Rincón *et al*. [48]. Alginic acid (as sodium salt) was obtained from Sigma-Aldrich and was used without further purification. All solvents used were HPLC grade and were from J.T. Baker. Potassium bromide (spectrophotometric grade) and silica gel 60 (230-400 mesh) were supplied by Merck.

**UV-Visible studies.** Spectra of the dyes in an aqueous solution were obtained in a Thermospectronic spectrophotometer (model Genesys 2) at different conditions:

a) Effect of pH: The different values of the dye solution were adjusted from acidic to basic values at a concentration of $1 * 10^{-5}$ M.
b) Effect of Dye Concentration in the absence and presence of the Biopolymer: The dye concentration was increased from 5 – 100 mg $L^{-1}$ at fixed values of pH and ionic strength corresponding to each dye in an aqueous solution in the presence of 1% (w/v) and in the absence of ALG to study the effect of this biopolymer on the dye aggregation phenomenon.
c) Effect of gelling agent: This procedure includes that described in b, but an additional step corresponding to the gel formation of ALG-Dye (Ca) product resulting from the addition of calcium chloride (5% w/v) to ALG-Dye solution.

In the cases of b and experiments, the pathlength of original cells was changed to adjust the absorbance to the detection limit of spectrophotometer, as a consequence, the response of the absorbance is not linear with the concentration values.

**Optimization of dye removal conditions.** The procedure used to determine the optimal conditions of dye removal was performed according to Jáuregui-Rincón *et al*. [48]. Briefly, each dye was dissolved in water and the concentration was adjusted to 250 ppm. An aliquot of this solution (40 mL) was added to a 50 mL solution of the biopolymer (1%). The pH of the samples was adjusted by using HCl and NaOH solutions. Three different pH values were evaluated: 4, 8, and 12. For each pH value, solutions with different ionic strength were prepared with the addition of sodium chloride crystals. The ionic strength values (I = 0.1M, 0.5M and 0.9M) were adjusted with a Corning Conductimeter checkmate II. The final volume of all samples was 100 mL and the final concentration of the dyes was 100 ppm (all samples were carried out in triplicate). Samples were cap sealed and shaken (200 rpm) for 24 h at 27 ºC in dark conditions.

Calcium chloride (30 mL of 5% w/v solution) was added to each sample in order to induce gel formation. Once the gel was formed, distilled water was added to complete final volume of 200 mL. All samples were kept at room temperature (27 ºC) for 24 h. The supernatant was centrifuged at 9000g for 20 min and free dye concentration was determined by UV-Vis spectroscopy.

## Application of Zimm-Bragg model to experimental Isotherms

The parameters of the Zimm-Bragg model for each system were obtained from experimental data and through the R statistical software [65]. The reported parameters in this investigation are optimal in the sense they minimize the sum of relative errors given by the equation 6:

$$L(K_u, u) = \sum_{i=1}^{n} \left( \frac{\beta - \hat{\beta}_i}{\beta_i} \right)^2 , \quad (6)$$

where $\beta_i$ is the i-th observed value and $\hat{\beta}_i$ represents the i-th theoretical value in the Zimm-Bragg model.

The optimization process was conducted in the R software by defining the loss function L(Ku, U) and by using the proposed values from experimental data as initial values.

**IR and Raman studies.** A sample powder of the pure dyes was used to obtain their corresponding Raman spectra. The analyzed powders (ALG-Dye (Ca) products) were isolated and purified as follows: The product was obtained from the last point of Removal isotherm (which contains the dye in the highest concentration in the gel). The product was separated by filtration, washed (five times with distilled water), dried (at 50 ºC during 60 h) and grounded. A MicroRaman system (Renishaw 1000) was used for Raman analysis (2000-400 $cm^{-1}$ range) and all samples were used without additional treatment.

For FT-IR the samples were analyzed (in a Perkin Elmer 1600 series) with potassium bromide pellets using transmission mode (systems including DR81 and DB22 dyes) and ATR mode (with a Thermo scientific Nicolet iS10, using a Germanium window) for DB1 systems in the 4000-650 range $cm^{-1}$.

## Acknowledgements

We gratefully acknowledged the support for this project by Consejo Nacional de Ciencia y Tecnología, México (CONACyT, GRANT No.9502). The authors wish to thank Dr. Carlos Peña-Malacara (Instituto de Biotecnología de la Universidad Nacional Autónoma de México) for the molecular weight determination of the biopolymer used in this work.

## References

1. Teng, T.T., Low, L.W. in: Advances in Water Treatment and Pollution. Sharma, S. K. and Sanghi, R. Eds. Springer, Dordrecht, **2012**, 65-93.
2. McMullan, G.; Meehan, C.; Conneely, A.; Kirby, N. *Appl. Microbiol. Biotechnol.* **2001**, *56*, 81-87.
3. Van der Zee, F.P.; Lettinga, G.; Field, J.A. *Chemosphere* **2001**, *44*, 1169-1176.
4. Junnarkar, N.; Srinivas-Murty, D.; Bhatt, N.S.; Madamwar, *D. World J. Microb. & Biot.* **2006**, *22*, 163-168.
5. Mondal, P. K., Chauhan, B. in: *Environmental Chemistry for a Sustainable World, Volume 2: Remediation of Air and Water Pollution*. Lichtfouse, E., Schwarzbauer, J. and Robert D. Ed; Springer, Dordrecht, **2012**, 255-275.
6. Tosik, R.; Wiktorowski, S. *Sci. Eng.* **2001**, *23*, 295-302.
7. Shu, H.Y.; Chang, M.C. *J. Hazard. Mater.* **2005**, *121*, 127-133.
8. Salama, T.M.; Ali, I.O.; Hanafya, A.I.; Al-Meligy, W.M. *Mater. Chem. Phys.* **2009**, *113*, 159-165.
9. Isaev A.B.; Aliev, Z.M.; Adamadzieva, N.A. *Russ. J. Appl. Chem.* **2012**, *85*, 765-769.
10. Ong, S.A.; Min, O.M.; Ho, L.N.; Wong, Y.S. *Water Air Soil Pollut.* **2012**, *223*, 5483–5493.
11. Genuino, H.C.; Hamal, D.B.; Fu, Y.J.; Suib, S.L. *J. Phys. Chem. C* **2012**, *116*, 14040-14051.
12. Pereira, L.; Alves, M. In: *Environmental Protection Strategies for Sustainable Development, Strategies for Sustainability*. Malik, A.; Grohmann, E. Ed; Springer, Dordrecht, **2012**, 111-162.
13. Ong, S.A.; Min, O.M.; Ho, L.N.; Wong, Y.S. *Environ. Sci. Pollut. Res.* **2013**, *20*, 3405–3413.
14. Yang, Z.; Lu, X.; Gao, B.; Wang, Y.; Yue, Q.; Chen, T. *J. Mater. Sci.* **2014**, *49*, 4962–4972.
15. Socha, A.; Sochocka, E.; Podsiadły, R. Sokołowska, J. *Color. Technol.* **2006**, *122*, 207–212.
16. Aquino, J.M.; Rodrigo, M.A.; Rocha-Filhoa, R.C.; Sáez, C.; Cañizares, P. *Chem. Eng. J.* **2012**, *184*, 221-227.
17. Horng, J.Y.; Huang, S.D. *Environ. Sci. Technol.* **1993**, *27*, 1169-1175.
18. Yilmaz, E.; Memon, S.; Yilmaz, M. *J. Hazard. Mater.* **2010**, *174*, 592-597.
19. Arslan, M.; Sayin, S.; Yilmaz, M. *Water Air Soil. Pollut.* **2013**, *224*, 1527-1536.
20. Yilmaz-Ozmen, E.; Erdemir, S.; Yilmaz, M.; Bahadir, M. *Clean* **2007**, *35*, 612-616.
21. Akceylan, E.; Bahadir, M.; Yılmaz, M. J. Hazard. Mater. **2009**, *162*, 960-966.

22. Kazakova, E.K.; Morozova, J.E.; Mironova, D.A.; Konovalov, A.I. *J. Incl. Phenom. Macrocycl. Chem.* **2012**, *74*, 467–472.
23. Kamboh, M.A.; Akoz, E.; Memon, S.; Yilmaz, M. *Water Air Soil Pollut.* **2013**, *224*,1424-1433.
24. Senan, R.C.; Abraham, T.E. *Biodegradation* **2004**, *15*, 275–280.
25. Parikh, A.; Madamwar, D. *Biotechnol. Lett.* **2005**, *27*, 323-326.
26. Arun-Prasad, A.S.; Satyanarayana, V.S.V.; Bhaskara-Rao, K.V. *J. Hazard. Mater.* **2013**, *262*, 674-684.
27. Reyes, P.; Pickard, M.A.; Vazquez-Duhalt, R. *Biotechnol. Lett.* **1999**, *21*, 875-880.
28. Liu, W.; Chao, Y.; Yang, X.; Bao, H.; Qian, S. *J. Ind. Microbiol. Biotechnol.* **2004**, *31*, 127–132.
29. Ramsay, J.A.; Mok, M.H.W.; Luu, Y.S.; Savage, M. *Chemosphere* **2005**, *61*, 956-964.
30. Guerrero, E.; Aburto, P.; Terrés, E.; Villegas, O.; González, E.; Zayas, T.; Hernández, F.; Torres, E. *J. Porous Mater.* **2013**, *20*, 387-396.
31. Arami, M.; Limaee, N.Y.; Mahmoodia, N.M.; Tabrizi, N.S.J. Hazard. Mater B **2006**, *135*, 171-179.
32. Aravindhan, R.; Fathima, N. N.; Rao, J. R.; Nair, B. U. Colloids Surf. A Physicochem. Eng. Asp. **2007**, *299*, 232-238.
33. Ferrero, F.; Periolatto, M. *Clean Techn. Environ. Policy* **2012**, *14*, 487-494.
34. Sanghi, R.; Bhattacharya, B. *Color. Technol.* **2002**, *118*, 256-269.
35. Annadurai, G. *Bioprocess Biosyst. Eng.* **2000**, *23*, 451-455.
36. Pal, M.K.; Mandal, N. *Biopolymers* **1990**, *29*, 1541-1548.
37. Blackburn, R.S. *Environ. Sci. Technol.* **2004**, *38*, 4905-4909.
38. Nasr, M.F.; El-Ola, S.M.A.; Ramadan, A.; Hashem, A.I. *Polym-Plast. Technol. Eng.* **2006**, *45*, 335-340.
39. Lozano-Alvarez, J. A.; Jáuregui-Rincón, J.; Mendoza-Díaz, G.; Rodríguez-Vázquez, R.; Frausto-Reyes, C. *J. Mex. Chem. Soc.* **2009**, *53*, 59-70.
40. Singh, V.; Malviya, T.; Sanghi, R. In: *Advances in Water Treatment and Pollution Prevention.* Sharma, S. K.; Sanghi, R. Eds. Springer, Dordrecht, **2012**, 377-403.
41. Braccini, I.; Perez, S. *Biomacromolecules* **2001**, *2*, 1089-1096.
42. Donati, I.; Holtan, S.; Mørch, Y.A.; Borgogna, M.; Dentini, M.; Skjåk-Bræk, M. *Biomacromolecules* **2005**, *6*, 1031-1040.
43. Oakes, J.; Dixon, S. *Rev. Prog. Color.* **2004**, *34*, 110-128.
44. Maurstad, G.; Danielsen, S.; Stokke, B.T. *J. Phys. chem. B* **2003**, *107*, 8172-8180.
45. Zimm, B.H.; Bragg, J.K. *J. Chem. Phys.* **1959**, *3*, 526-535.
46. Schwarz, G.; Balthasar, W. Eur. J. Biochem. **1970**, *12*, 461-467.
47. Satake, I.; Yang, J.T. *Biopolymers* **1976**, *15*, 2263-2275.
48. Jáuregui-Rincón, J.; Lozano-Alvarez, J.A.; Medina-Ramírez, I. In: Elnashar, M. Ed. *Biotechnology of Biopolymers*, Intech, Croacia, **2011**, 165-190.
49. Lindstrom, T.; Christer, S. *J. colloid. Interf. Sci.* **1976**, *55*, 69-72.
50. Singh, R.P.; Tripathy, T.; Karmakar, G.P.; Rath, S.K.; Karmakar, N.C.; Pandey, S.R.; Kannan, K.; Jain, S.K.; Lan, N.T. *Curr. Sci.* **2000**, *78*, 798-803.
51. Retes-Pruneda, J.L.; Davila-Vazquez, G.; Medina-Ramírez, I.; Chavez-Vela, N.A.; Lozano-Alvarez, J.A.; Alatriste-Mondragon, F.; Jauregui-Rincon, J. *Environ. Technol.* **2014**, *35*, 1773-1784.
52. Abbott, L.C.; Batchelor, S.N.; Jansen, L.; Oakes, J.; Lindsay-Smith J.R., Moore, J,N, *New. J. Chem.* **2004**, *28*, 815-821.
53. Monahan, A.R.; Blossey, D.F. *J. Phys. Chem.* **1971**, *75*, 1227-1233.
54. Reeves, R.L.; Maggio, M.S.; Harkaway, S.A.A. *J. Phys. Chem.* **1979**, *83*, 2359-2368.
55. Hamada, K.; Mitshuishi, M.; Ohira, M.; Miyazaki, K. *J. Phys. Chem.* **1993**, *97*, 4926-4929.
56. Tiddy, G.J.T.; Mateer, D.L.; Ormedrod, A.P.; Harrison, W.J.; Edwards, D.J. *Langmuir* **1995**, *11*, 390-393.
57. Ferus-Camelo, M.; Greaves, A.J. *Color. Technol.* **2002**, *118*, 15-19.
58. Abbot, L.C.; Batchelor, S.N.; Oakes, J.; Lindsay-Smith, J.R., Moore, J.N. *J. Phys. Chem. B* **2004**, *108*, 13726-13735.
59. Yoshida, Z.I.; Osawa, E.; Oda, R. *J. Phys. Chem.* **1964**, *68*, 2895-2898.
60. Abbott, L.C.; Batchelor, S.N.; Oakes, J.; Lindsay-Smith, J.R.; Moore, J.N. *J. Phys. Chem. A* **2004**, *108*, 10208-10218.
61. Abbott, L.A.; Batchelor, S.N.; Oakes, J.; Gilbert, B.C.; Whitwood, A.C.; Lindsay-Smith, J.R.; Moore, J.N. *J. Phys. Chem. A* **2005**, *109*, 2894-2905.
62. Silverstein, R.; Milton, R. *Spectrometric Identification of Organic Compounds*. Fifth ed. John Wiley & sons, USA, 1991, 127.
63. Armstrong, D.R.; Clarkson, J.; Smith, W.E. *J. Phys. Chem.* **1995**, *99*, 17825-17831.
64. Biswas, N.; Umapathy, S. *J. Phys. Chem. A* **2000**, *104*, 2734-2745.
65. Core, R. T. R: A language and Environment for statistical computing. R Foundation for Statistical Computing, Vienna, Austria, **2013**, http: //www.R-project.org.